

## Chapter 2

### Ammonia Chemisorption on Well-Defined SnO<sub>2</sub> (110) Surfaces

#### 2.1. Introduction

The use of probe molecules, such as ammonia, pyridine, and carbon dioxide, to characterize acid/base properties of oxide surfaces is common in catalysis, and the relationship between acid/base properties and the observed chemistry is often investigated to give insight into the nature of oxide reactivity [1]. For example, in the oxidation of methanol to formaldehyde over MoO<sub>3</sub>-SnO<sub>2</sub> and SnO<sub>2</sub>-K<sub>2</sub>O, mixed oxide catalysts, formaldehyde production is thought to be associated with surface acidity, while CO<sub>2</sub> production is associated with surface basicity [2].

The nature of acidic and basic sites on oxide surfaces can be described in Lewis and Brønsted terms. For clean metal oxide surfaces (no surface protons), the properties are principally described in terms of Lewis acidity and basicity. On metal oxides, coordinately unsaturated metal cations are generally thought to be Lewis acid sites, while the oxygen anions are thought to be Lewis base sites [3]. The electron-deficient metal cations exhibit acidic, electron-acceptor character, while the electron-rich oxygen anions exhibit basic, electron-donor character [4].

A molecular view of the relationship between the Lewis acidity and basicity of metal oxide surfaces has proven useful in studying the chemistry of well-defined oxide systems. Vohs and Barteau showed that cation/anion accessibility is required for the

dissociation of Brønsted acids on single crystal ZnO surfaces [5]. The (0001)-Zn polar surface exposes oxygen anions and zinc cations that provide the acid/base site pair necessary to dissociatively adsorb many Brønsted acids. The (0001)-O polar surface is terminated by oxygen anions that sterically block the zinc cations. This anion-terminated surface is inert with respect to dissociation of Brønsted acids because there are no accessible cations to form the acid/base site pairs [5-11].

$\text{SnO}_2$  (110) is a useful model for defective oxide surfaces because of the flexibility it allows in controlling cation coordination numbers, oxidation states, and the formation (i.e., intentional introduction) of two different types of surface oxygen vacancies [12-14]. The oxidation of a number of molecules has been studied over  $\text{SnO}_2$ (110), and the chemistry has been found to be dependent on the surface condition. For methanol, the initial dissociation reaction to form surface methoxide was found to be controlled by the availability of specific surface cations [15]. While anions and coordinately-unsaturated cations were available on all the surfaces studied, the results indicated that the type of cation associated with the site/pair was critical for the dissociation of methanol and hence in defining the surface chemistry. However, this observed dissociation behavior of methanol is not well understood. In particular, the relationship between local surface properties and the acid/base properties of the site pairs remains undefined.

In the present work, the chemisorption of a standard basic probe molecule, ammonia, has been examined over  $\text{SnO}_2$  (110). The first aim of the study is to understand the details of the interaction of ammonia at specific, well-defined defect sites on an oxide surface. The second goal of the study is to use a standard characterization of the acidity

of different cation sites with the goal of determining whether a simple acid/base description is applicable to the previous results for methanol dissociation [15].

## 2.2 Experimental

For TDS experiments, all surfaces were exposed to  $\text{NH}_3$  at 190 K and heated to 650 K using a linear temperature ramp of 2 K/sec. During TDS experiments, the background pressure was less than  $2 \times 10^{-10}$  Torr between doses. For all UPS experiments, all surfaces were exposed to  $\text{NH}_3$  also at 190 K.

## 2.3 Results

### 2.3.1 *Thermal Desorption Spectroscopy*

TDS of  $\text{NH}_3$  can be thought of as a way to provide a measure of the strength of the Lewis acidity of cations associated with specific sites. Variations in  $\text{NH}_3$  adsorption were examined by TDS for all the surface preparations described above. All surfaces were exposed to  $\text{NH}_3$  at 190 K and heated linearly at 2 K/sec to 650 K. All desorption features are thought to be first-order and originate from a molecular  $\text{NH}_3$  adsorbate. Only  $\text{NH}_3$  was observed in TDS following  $\text{NH}_3$  adsorption. Desorption of  $\text{H}_2$ ,  $\text{H}_2\text{O}$ , and  $\text{N}_2$  was checked for but not observed in TDS. The lack of reaction products suggests no dissociation of  $\text{NH}_3$ . A second-order Redhead analysis of the TDS data shows no linearity suggestive of second-order behavior that might indicate a  $\text{NH}_3$  recombination process [16]. Additionally, UPS data in section 2.3.3.2 supports the idea that the adsorption of ammonia is molecular.

### ***2.3.1.1 Nearly-stoichiometric surface (oxidized)***

The coverage dependence of the NH<sub>3</sub> desorption traces from a clean, nearly-stoichiometric surface is illustrated in Figure 2.1 (a). At the lowest dose investigated, 0.02 L (1L=10<sup>-6</sup> Torr-sec), one NH<sub>3</sub> desorption peak is observed with a peak maximum at 290 K. This feature shifts down in temperature to 255 K with increasing coverage. On metal oxide surfaces, metal cations are thought of as Lewis acid sites [4]. Since the nearly-stoichiometric surface exposes predominately five-coordinate Sn<sup>4+</sup> cations, the NH<sub>3</sub> TDS feature is attributed to the adsorption of basic NH<sub>3</sub> molecules at five-coordinate Sn<sup>4+</sup> cations. Assuming a pre-exponential of 10<sup>13</sup> s<sup>-1</sup>, a range of 15.9-18.1 kcal/mol for the first-order activation energy for desorption can be calculated from the Redhead equation [17]. No attempt was made to independently determine the pre-exponential via the method of heating rate variation. The heating rate was kept intentionally low (2 K/sec) to avoid the possibility of thermal fracture of the ceramic sample.

### ***2.3.1.2 Reduced surface (oxidized, 700K-annealed)***

The coverage dependence of the NH<sub>3</sub> desorption traces on the “reduced” surface is illustrated in 2.1 (b). At the lowest dose investigated, 0.02 L, a NH<sub>3</sub> desorption feature is observed at 470 K. With increasing coverages, a second NH<sub>3</sub> feature appears at 320 K for doses as low as 0.05 L. The higher-temperature feature remains at 470 K while the lower-temperature feature shifts to lower temperatures (down to 295 K) with increasing exposures (up to 0.38 L). The apparent first-order activation energy for desorption is

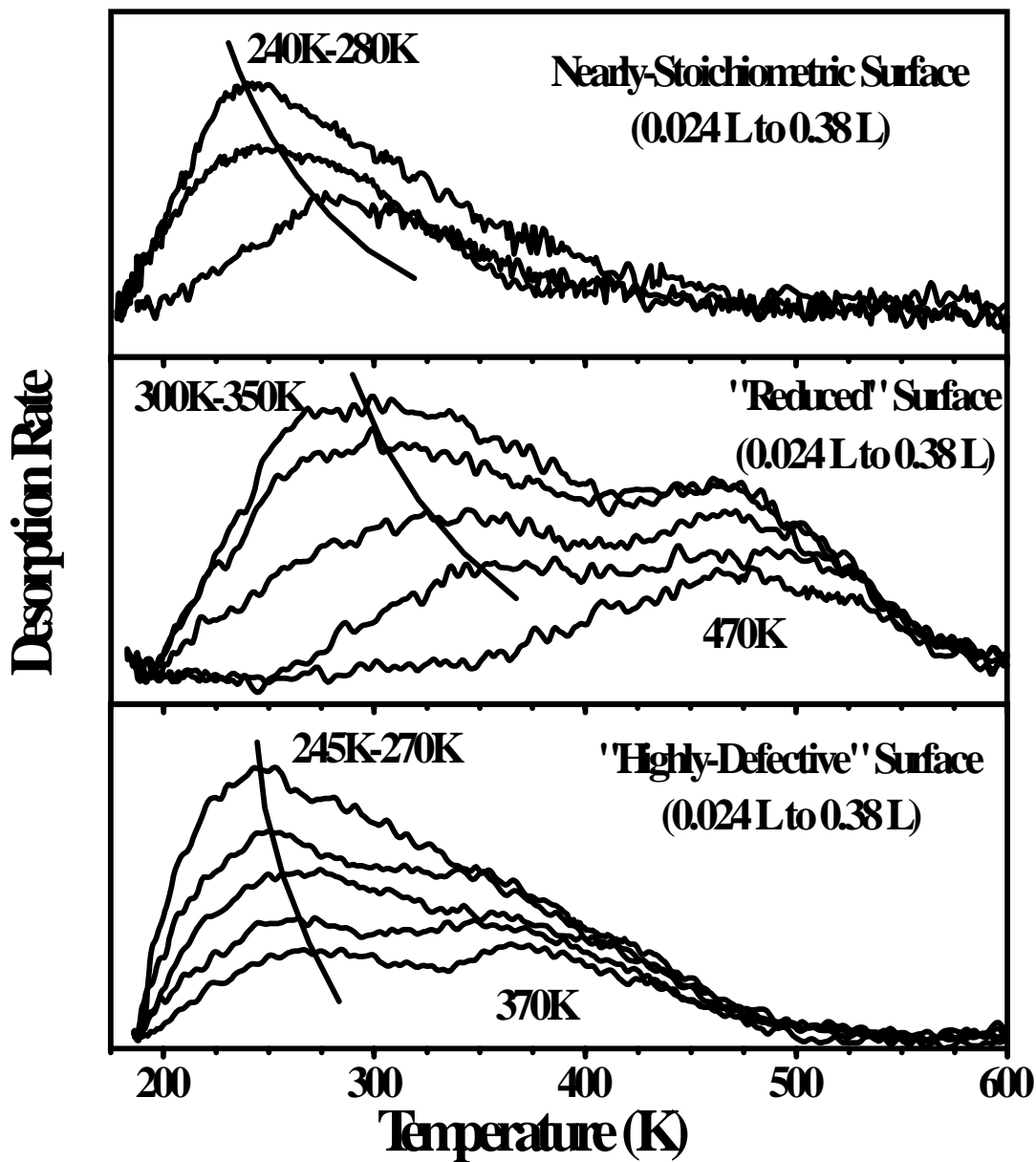


Figure 2.1 Ammonia TDS traces following adsorption at exposures of 0.02 L to 0.38 L at 190 K on SnO<sub>2</sub> (110): nearly-stoichiometric surface (top), “reduced” surface (middle), and “highly-defective” surface (bottom).

29.8 kcal/mol for the 470 K feature and 18.5-20.1 kcal/mol for the lower temperature feature [16]. Since the 470 K feature appeared with the exposure of  $\text{Sn}^{2+}$  cations on the “reduced” surface, the 470 K feature is attributed to the desorption of molecular  $\text{NH}_3$  from four-coordinate  $\text{Sn}^{2+}$  cations associated with bridging oxygen vacancies. As was seen on the nearly-stoichiometric surface, the lower-temperature 295-320 K feature is attributed to  $\text{Sn}^{4+}$  cations. Note that this feature associated with five-coordinate  $\text{Sn}^{4+}$  cations at 295-320 K on the "reduced" surface appears at a higher temperature than on the nearly-stoichiometric surface (255-290 K). The difference in temperatures in TDS between these two surfaces will be discussed in section 2.4.4.

### 2.3.1.3 “Highly-Defective” surface

The coverage dependence of the  $\text{NH}_3$  desorption traces on a "highly-defective" surface is illustrated in 2.1 (c). Two desorption features are observed, similar to those from the “reduced” surface, but they are shifted to lower temperatures upon the introduction of in-plane oxygen vacancies. At the lowest dose investigated, 0.02 L, two desorption features are observed at 250 K and 365 K. An activation energy of desorption of 15.6 kcal/mol is calculated for the lower-temperature feature and 23.0 kcal/mol for the higher-temperature feature [16]. The lower-temperature feature is attributed to the reduced coordination cations that were originally five-coordinate  $\text{Sn}^{4+}$  cations before the introduction of in-plane oxygen vacancies. The higher-temperature feature is attributed to the reduced coordination cations that were originally four-coordinate  $\text{Sn}^{2+}$  cations before the introduction of in-plane oxygen vacancies. The differences in temperatures between the “reduced” and “highly-defective” surfaces will be discussed in section 2.4.5.

### 2.3.2 He I UPS measurements

#### 2.3.2.1 Changes in surface electronic properties upon adsorption

He I UPS was used on all SnO<sub>2</sub> surfaces to study changes in surface electronic properties upon adsorption. An example of a He I spectrum for a “highly-defective” SnO<sub>2</sub> (110) surface is shown in Figure 2.2. Changes in work function were measured by shifts in the vacuum level cutoff of the He I spectra. A shift to lower binding energies show an increase in the work function ( $\phi$ ), while a shift to higher binding energies is a decrease in work function. For a semiconductor, these changes in the work function ( $\Delta\phi$ ) include contributions due to band bending ( $-e\Delta V_s$ ) and changes in the surface dipole ( $\Delta\chi$ ) according to the relationship,  $\Delta\phi = \Delta\chi - e\Delta V_s$  [17]. Band bending changes were determined from the shifts in the low-binding energy edge of the substrate features near the valence band maximum, where a shift to higher binding energies is characteristic of downward band bending (a positive  $V_s$ ) and accumulation of electrons in the space charge layer. The change in surface dipole was calculated from the work function and band bending changes. A positive surface dipole ( $\chi$ ) ( $- \rightarrow +$ ) is oriented into the surface.

Changes in work function, band bending, and surface dipole relative to a clean, nearly-stoichiometric surface are shown in Figure 2.3 as a function of dose for NH<sub>3</sub> adsorption at 193 K. Figure 2.3 shows decreases in the work function, downward band bending, and decreases in the surface dipole for all surfaces. The largest contribution to changes in the work function is accounted for by the surface dipole. The surface dipole

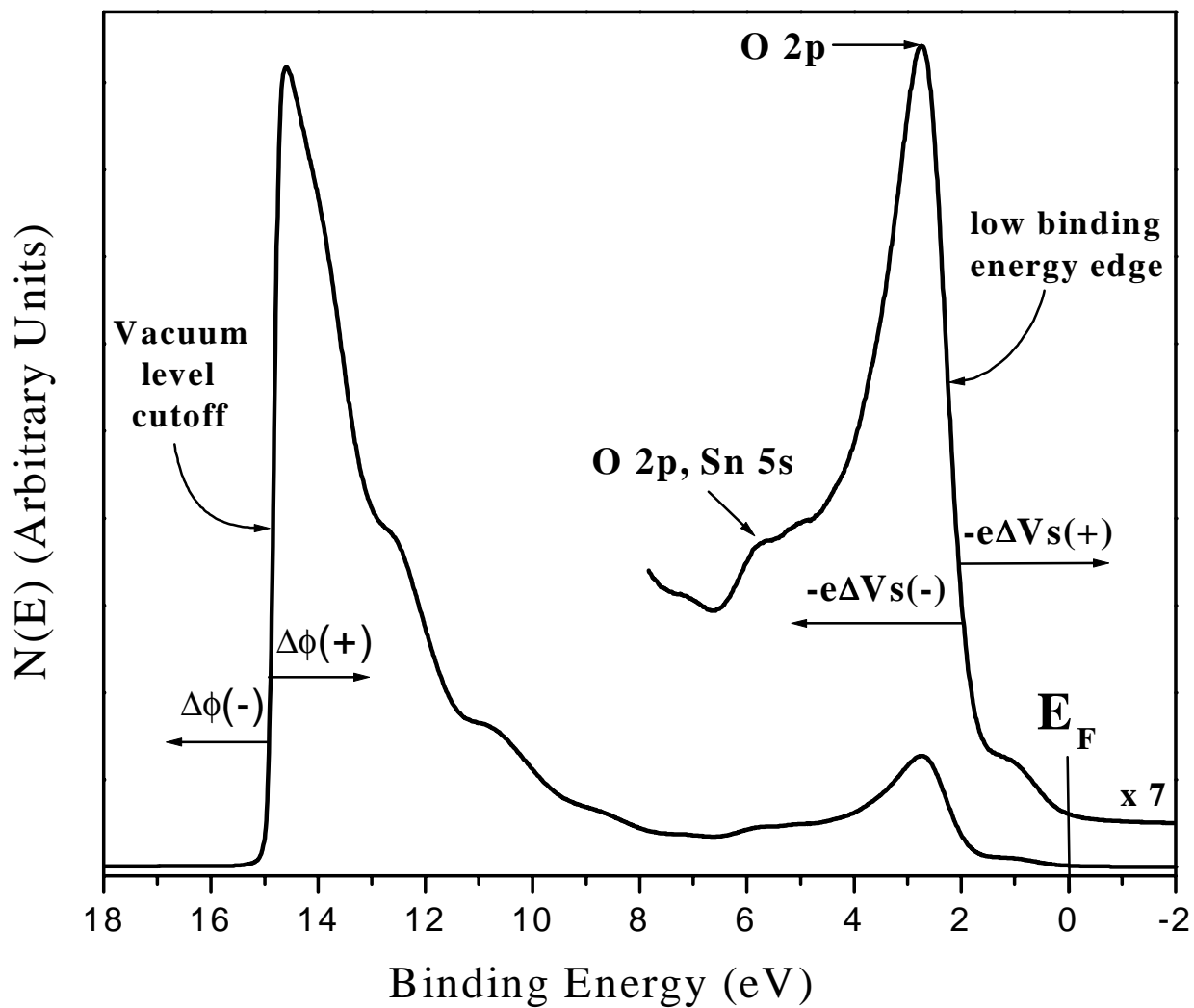


**Figure 2.2** He I UPS spectrum of a “highly-defective” SnO<sub>2</sub> (110) surface used to measure changes in the surface dipole ( $\Delta\chi$ ), band bending ( $-e\Delta V_s$ ), and work function ( $\Delta\phi$ ).

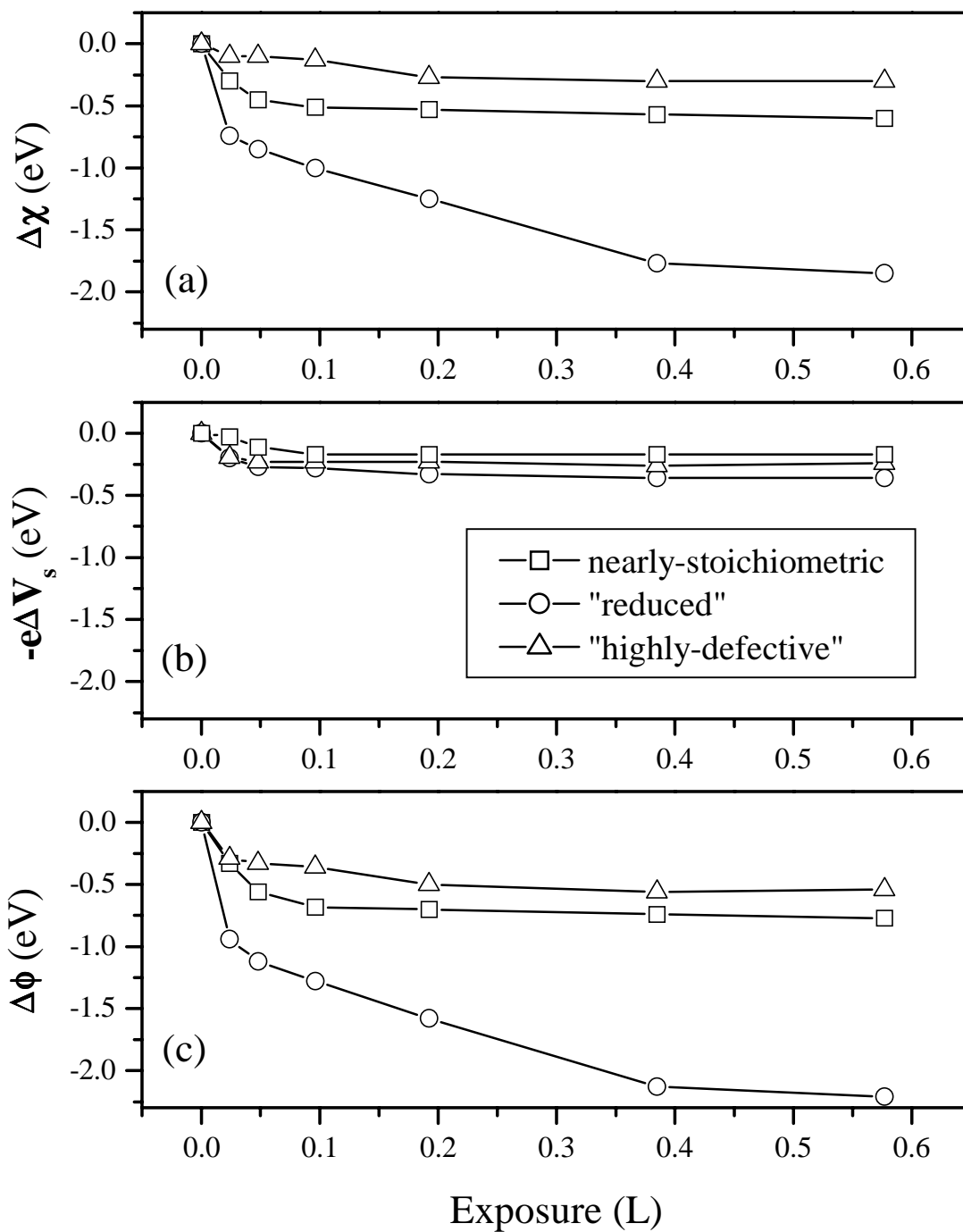


**Figure 2.3** He I UPS spectra showing variations in: (a) surface dipole,  $\Delta\chi$ , (b) band bending,  $-e\Delta V_s$ , and (c) work function,  $\Delta\phi$ . All spectra are a function of dose for the nearly-stoichiometric, “reduced”, and “highly-defective” SnO<sub>2</sub> (110) surfaces.

decreases with increasing exposures up to 0.38 L for all surfaces (shown in Figure 2.3), and indicates that saturation of the surface by NH<sub>3</sub> is achieved by 0.38 L. A decrease in the surface dipole upon NH<sub>3</sub> adsorption indicates that charge is transferred from the NH<sub>3</sub> molecules to the surface, suggesting the NH<sub>3</sub> molecules bind to the surface via the nitrogen lone pair. The surface dipole is positively oriented into the surface. The decrease in surface dipole of the nearly-stoichiometric surface is 0.57 eV at saturation. For the "reduced" surface, the change in dipole is the largest, decreasing by 1.77 eV at saturation. For the "highly-defective" surface, the smallest change in dipole is observed at saturation, a 0.30 eV decrease.

From the variation in  $-e\Delta V_s$ , it is apparent that the bands bend down with increasing NH<sub>3</sub> exposures for all surfaces (shown in Figure 2.3). SnO<sub>2</sub> is a n-type semiconductor [12]. The downward band bending indicates an accumulation of electrons in the space charge layer associated with the donation of electrons from the NH<sub>3</sub> molecule to the surface. At saturation, the smallest amount of band bending (0.17 eV) is seen for the nearly-stoichiometric surface. For the "reduced" surface, the largest amount of band bending (0.36 eV) is observed at saturation. An intermediate degree of band bending (0.24 eV) is seen for the "highly-defective" surface.

### ***2.3.2.2 Coverage estimates***

To estimate the coverage of NH<sub>3</sub> molecules on the surface, the NH<sub>3</sub> flux is first estimated from the kinetic theory of gases [17]. Assuming a sticking coefficient of unity up to saturation, 0.38 L, allows an upper-limit estimate of the coverage of  $1.9 \times 10^{14}$  NH<sub>3</sub> molecules/cm<sup>2</sup>. The number of Sn sites on each surface can be estimated from the unit

cell parameters [13]. The nearly-stoichiometric surface is estimated to expose  $4.7 \times 10^{14}$  five-coordinate  $\text{Sn}^{4+}$  sites/ $\text{cm}^2$ . The “reduced” surface exposes an additional equal number of  $4.7 \times 10^{14}$  four-coordinate  $\text{Sn}^{2+}$  sites/ $\text{cm}^2$  due to the removal of bridging oxygen anions. The number of Sn cations exposed to the “highly-defective” surface is not expected to change significantly with the introduction of in-plane oxygen vacancies. A fractional coverage is calculated by taking the estimated coverage of  $\text{NH}_3$  molecules on the surface and dividing by the total number of Sn cations exposed on the surface. The “highly-defective” surface shows the largest  $\text{NH}_3$  uptake of any surface. Using the upper-limit coverage estimate for the “highly-defective” surface, a fractional coverage of 0.20 is calculated. The nearly-stoichiometric surface has a third of the coverage of the “highly-defective” surface and half the number of exposed Sn cations. Therefore, a fractional coverage of 0.13 is found for the nearly-stoichiometric surface. The “reduced” surface has three-fourth of the  $\text{NH}_3$  coverage of the “highly-defective” surface resulting in a fractional coverage of 0.15. The fractional coverages on all surfaces are smaller than expected. Repulsive lateral interactions between  $\text{NH}_3$  molecules probably limit the  $\text{NH}_3$  uptake. Evidence for repulsive interactions is shown in TDS by the decreasing activation energies of desorption with increasing  $\text{NH}_3$  coverages.

### ***2.3.2.3 Charge transfer estimates***

The amount of charge transfer from the adsorbate to the surface can be estimated from the band bending changes ( $\Delta V_s$ ) using a standard parallel-plate capacitor model for the semiconductor space charge layer in which the presence of a localized charged layer at

the surface is attributed to surface states. The space charge density,  $Q_{sc}$ , is the total net charge in the space-charge region per unit area given by the equation:

$$Q_{sc} = -e \times n_b \times L \times F_s.$$

Where  $e$  is the absolute magnitude of electronic charge,  $n_b$  is the bulk carrier density,  $L$  is the effective Debye length, and  $F_s$  is a space charge function at the surface [18]. The bulk carrier density,  $n_b$ , is estimated from

$$n_b = \sigma / (e \times \mu)$$

to be  $1.25 \times 10^{10} \text{ cm}^{-3}$  for the expected conductivity,  $\sigma$ , of  $\text{SnO}_2$  ( $10^{-6} \Omega^{-1} \text{ cm}^{-1}$  [19]), and the Hall mobility,  $\mu$ , at 180 K ( $500 \text{ cm}^2 \text{ V}^{-1} \text{ sec}^{-1}$  [19]). The effective Debye length,  $L$ , is estimated to be  $3.10 \times 10^{-2} \text{ cm}$  from:

$$L = [(\epsilon \times \epsilon_0 \times k \times T) / (e^2 \times n_b)]^{1/2}$$

where  $\epsilon$  is the dielectric constant of  $\text{SnO}_2$  (14 [20]),  $\epsilon_0$  is the permittivity of free space,  $k$  is the Boltzmann's constant, and  $T$  is the temperature [18].  $F_s$  is given by:

$$F_s = \sqrt{2} [ \exp(|V_s|) - |V_s| - 1 ]^{1/2} \text{ for } V_s > 0.$$

where  $V_s$  is the surface potential. Assuming the nearly-stoichiometric surface represents the flat band position where the surface potential is zero, the surface potential,  $V_s$ , may be taken directly from the amount of band bending,  $-e\Delta V_s$  [18]. From the He I data, the band bending at saturation is  $-0.17 \text{ eV}$  for the nearly-stoichiometric surface,  $-0.36 \text{ eV}$  for the "reduced" surface, and  $-0.24 \text{ eV}$  for the "highly-defective" surface relative to the clean nearly-stoichiometric surface. The surface state charge density is equal to the negative of the space charge density:

$$Q_{ss} = -Q_{sc},$$

and the induced charge per adsorbed ammonia molecule can be estimated from Gauss's law:

$$q = Q_{ss}/(e \times n_s^{\text{ads}})$$

where  $n_s^{\text{ads}}$  is the number of adsorbed  $\text{NH}_3$  molecules per unit area [18]. The upper-limit number of  $\text{NH}_3$  molecules at saturation is  $1.9 \times 10^{14}$   $\text{NH}_3$  molecules/ $\text{cm}^2$ . Using this upper-limit estimate for the "reduced" and "highly-defective" surfaces, the amount of charge transfer per  $\text{NH}_3$  molecule is estimated at saturation to be  $3.15 \times 10^{-1}$  electrons per molecule for the "reduced" surface and  $6.60 \times 10^{-3}$  electrons per molecule for the "highly-defective" surface. The nearly-stoichiometric surface has only  $\text{Sn}^{4+}$  cations exposed to the surface. Therefore, the upper-limit estimate of coverage is decreased by half for the nearly-stoichiometric surface resulting in an amount of charge transfer per  $\text{NH}_3$  molecule at saturation to be  $6.92 \times 10^{-4}$  electrons per molecule.

The absolute values calculated for charge transfer,  $q$ , are less important than the comparison of charge transfer between the different  $\text{SnO}_2$  surfaces. There are noticeable differences in coverages between the different  $\text{SnO}_2$  surfaces, but this does not affect the overall trend of charge transfer between the surfaces. For instance, the upper-limit estimate of coverage is decreased by half on the nearly-stoichiometric surface due to only having  $\text{Sn}^{4+}$  cations exposed, and the charge transfer per molecule is only doubled. The charge transfer calculated for the nearly-stoichiometric surface is still an order of magnitude smaller than the charge transfer calculated for the "highly-defective" surface.

Charge transfer calculations on the "reduced" surface using UPS band bending measurements have contributions averaged from two different adsorption states associated with  $\text{Sn}^{2+}$  and  $\text{Sn}^{4+}$  cations in TDS. On the nearly-stoichiometric surface, UPS probes only

the  $\text{Sn}^{4+}$  sites that are exposed. Assuming the  $\text{Sn}^{4+}$  sites on the “reduced” surface do not differ much from the nearly-stoichiometric surface, the large charge transfer increase from the nearly-stoichiometric surface to the “reduced” surface likely comes predominantly from the  $\text{NH}_3$  adsorbed at four-coordinate  $\text{Sn}^{2+}$  sites on the “reduced” surface.

### **2.3.3 He II UPS measurements**

#### **2.3.3.1 Condensed $\text{NH}_3$**

He II UPS was used to investigate the electronic states of adsorbed  $\text{NH}_3$  because of the small inelastic background compared to He I UPS. The assignment of the electronic states of adsorbed  $\text{NH}_3$  on  $\text{SnO}_2$  (110) was made by comparing the spectra of condensed and gas phase  $\text{NH}_3$ .  $\text{NH}_3$  condensed on  $\text{SnO}_2$  should resemble molecular gas phase  $\text{NH}_3$ .  $\text{NH}_3$  was condensed on  $\text{SnO}_2$  (110) at 140 K by exposing  $\text{NH}_3$  to the surface at a constant pressure of  $10^{-6}$  Torr. The resulting He II UPS spectrum shown in Figure 2.4 is similar to that observed for He I spectrum of gas-phase  $\text{NH}_3$  by Turner *et al.* (reproduced in Figure 2.4) [21]. In the He II spectrum, two features with a splitting of 5.4 eV are observed at binding energies of 1.5 eV and 6.9 eV. Comparison to the electronic structure of gas phase  $\text{NH}_3$  allows the assignment of the higher binding energy feature to the  $1e$  molecular orbital associated with the molecular N-H bonds and the lower binding energy feature to the  $3a_1$  molecular orbital representative of the lone pair on the nitrogen atom [22].

#### **2.3.3.2 Chemisorbed $\text{NH}_3$**

UPS experiments were conducted following 0.77 L exposures of  $\text{NH}_3$  at 193 K. This exposure was sufficient to saturate the surface, as indicated by the He I UPS data. He

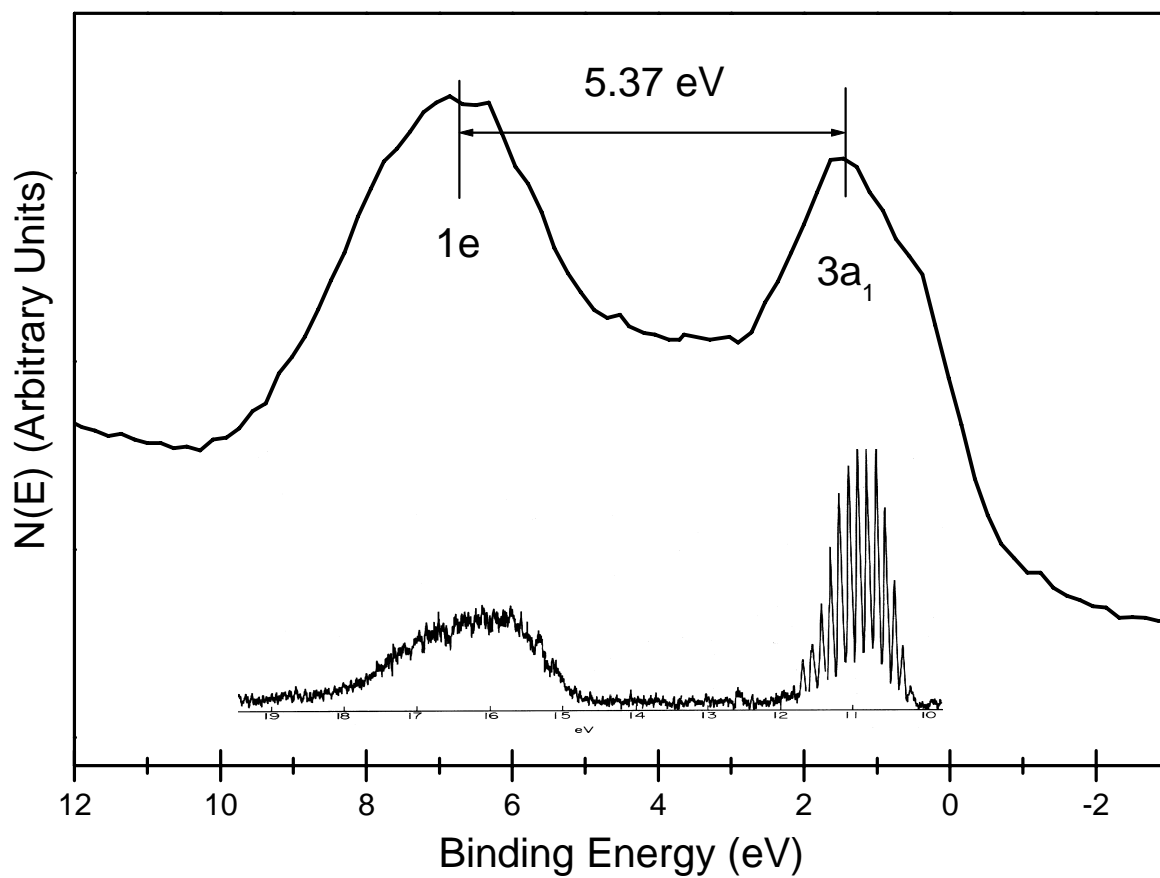


**Figure 2.4** He II UPS spectra of condensed NH<sub>3</sub> on SnO<sub>2</sub> (110) at 140 K and a constant pressure of 10<sup>-6</sup> Torr NH<sub>3</sub>. A He I UPS spectra of gas-phase NH<sub>3</sub> by Turner, *et al.* has been reproduced for comparison.

II difference curves shown in Figure 2.5 were generated by normalization and alignment of the clean and NH<sub>3</sub> dosed spectra on substrate features near the valence band maximum to account for band bending. Two NH<sub>3</sub> induced features corresponding to the 1e and 3a<sub>1</sub> MOs of molecular NH<sub>3</sub> are observed in the difference spectra on all surfaces, suggesting primarily a molecular adsorption process.

For the nearly-stoichiometric surface, two features corresponding to the 1e and 3a<sub>1</sub> MOs of molecular NH<sub>3</sub> appear at binding energies of 6.3 eV and 2.6 eV (Figure 2.5). The “reduced” and “highly-defective” surfaces exhibit two features at binding energies of 6.3 eV and 3.4 eV (shown in Figure 2.5). In all cases, the 1e-3a<sub>1</sub> splitting for chemisorbed NH<sub>3</sub> is less than the 5.4 eV observed for condensed and gas phase NH<sub>3</sub> (Figure 2.4). The nearly-stoichiometric surface has a 3a<sub>1</sub>-1e splitting of 3.7 eV while the “reduced” and “highly-defective” surfaces have a 3a<sub>1</sub>-1e splitting of 2.9 eV.

Since the primary adsorbate-surface interaction should occur through the lone pair on the nitrogen atom in NH<sub>3</sub>, the decreases in 3a<sub>1</sub>-1e splitting relative to the gas-phase is interpreted as a relaxation of the 3a<sub>1</sub> lone-pair orbital. The 1e  $\pi$  molecular orbital of ammonia associated with N-H bonds should be little affected by chemisorption. Lin *et al.* [23] used CuCl and ZnO as a comparison to study the  $\sigma$ -bonding interaction between the unoccupied metal 4s and 4p orbitals and the NH<sub>3</sub> 3a<sub>1</sub> lone pair molecular orbital on nitrogen by using the stabilization of the 3a<sub>1</sub> MO in He II UPS. X- $\alpha$  calculations indicated that cation d character in the chemisorption bond can change the 3a<sub>1</sub> orbital energy [23]. However, in our study, comparisons are made between the same metal oxide, SnO<sub>2</sub> (110). Therefore, differences due to cation d orbital interactions should be small. Therefore, a

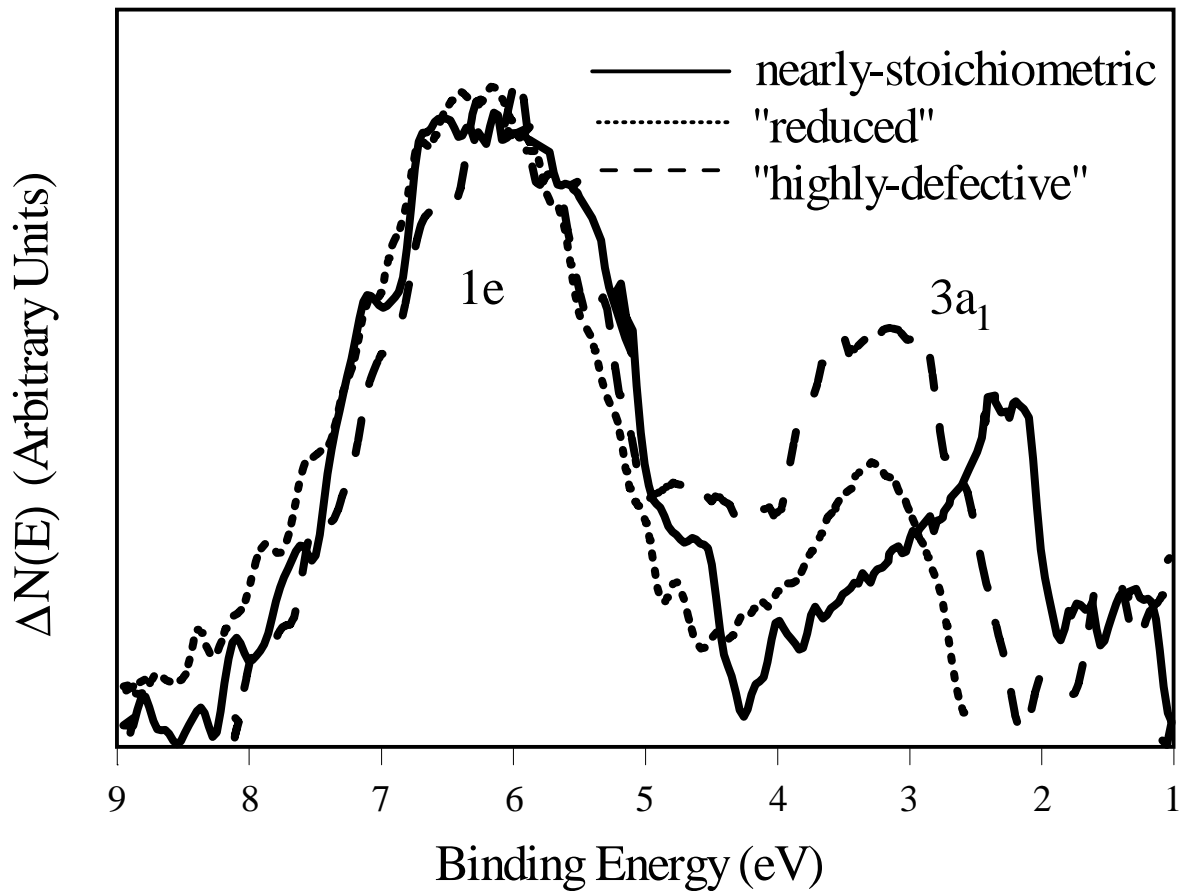


**Figure 2.5** He II UPS difference spectra for NH<sub>3</sub> adsorbed at 193 K on the nearly-stoichiometric, “reduced”, and “highly-defective” SnO<sub>2</sub> (110) surfaces. The N(E) curves are characteristic of molecular NH<sub>3</sub>.

greater stabilization of the ammonia  $3a_1$  orbital represents a greater degree of covalency in the chemisorption bond. The covalent bonding of ammonia to the surface, probed by the stabilization of the  $3a_1$  energy, is attributed to a sigma-bonding interaction between the unoccupied Sn cation 5s and 5p orbitals and the ammonia  $3a_1$  lone pair molecular orbital on nitrogen.

Measurements of the  $3a_1$  stabilization on the nearly-stoichiometric surface have contributions from only the  $\text{Sn}^{4+}$  cations exposed on this surface. On the “reduced” surface, UPS probes both the  $\text{Sn}^{2+}$  and  $\text{Sn}^{4+}$  sites that are exposed. The  $\text{Sn}^{4+}$  sites on the “reduced” surface should not differ much from the nearly-stoichiometric surface. Therefore, two  $3a_1$  features on the “reduced” surface are expected, one from the  $\text{Sn}^{2+}$  sites and one from the  $\text{Sn}^{4+}$  sites. But only the  $3a_1$  feature for the  $\text{Sn}^{2+}$  sites is seen on the “reduced” surface.

## 2.4 Discussion

### 2.4.1 Lewis acidity of Sn cations

In terms of its electronic structure,  $\text{NH}_3$  can be thought of as a straight forward probe for Lewis acidity. The  $3a_1$  lone pair MO on the nitrogen atom acts as a  $\sigma$  donor. The lowest unoccupied  $4a_1$  and  $2e$  molecular orbitals lie well above the vacuum level, hence  $\pi$ -backbonding contributions may be neglected [24]. Therefore,  $\text{NH}_3$  should be a useful probe molecule of the  $\sigma$  acceptor function of a surface cation. If the strength of the interaction of  $\text{NH}_3$  with a cation is taken as a measure of the Lewis acidity of the cation,  $\text{NH}_3$  chemisorption indicates that the four-coordinate  $\text{Sn}^{2+}$  cations are stronger acidic sites than five-coordinate  $\text{Sn}^{4+}$  cations. Assuming the adsorption of  $\text{NH}_3$  is unactivated, the

activation energies of  $\text{NH}_3$  desorption are equivalent to the heats of adsorption, the heat of  $\text{NH}_3$  adsorption at the  $\text{Sn}^{2+}$  cations exposed on the “reduced” surface is 29.8 kcal/mol which is greater than the heat of  $\text{NH}_3$  adsorption at the five-coordinate  $\text{Sn}^{4+}$  cations, 15.9-20.1 kcal/mol, on both the “reduced” and nearly-stoichiometric surfaces.

#### **2.4.2 Bonding of $\text{NH}_3$**

A chemical bond can generally be considered in terms of ionic and covalent contributions. For the adsorption of  $\text{NH}_3$  at a cation site, the ionic contribution can be thought of as an ion-dipole interaction. If the ion-dipole interactions dominate, the cations with the highest oxidation state should be the strongest binding site. In TDS from the “reduced” surface, the higher temperature feature corresponds to adsorption at  $\text{Sn}^{2+}$  cations not  $\text{Sn}^{4+}$  cations. The ordering suggests that covalent interactions dominate over the ion-dipole interaction. The covalent interaction can be thought of as Sn 5s and 5p related bands accepting electron density from the  $3a_1$  lone pair orbitals on the nitrogen atom of  $\text{NH}_3$ .

Changes in electronic properties of  $\text{SnO}_2$  and  $\text{NH}_3$  upon adsorption give an indication that  $\text{NH}_3$  forms covalent bonds to the Sn cations. The decrease in the surface dipole indicates charge transfer to the surface, band bending measurements yield an estimate of the amount of charge transfer, and the  $3a_1$  stabilization observed in UPS gives a qualitative indication of the strength of the covalent interaction between Sn cations and  $\text{NH}_3$  molecules. A greater decrease in surface dipole, charge transfer between  $\text{NH}_3$  and the surface, and  $3a_1$  stabilization are seen when  $\text{Sn}^{2+}$  cations are exposed on the “reduced” surface. These differences suggest a greater covalent bonding interaction between the  $\text{NH}_3$

molecule and the exposed four-coordinate  $\text{Sn}^{2+}$  cation sites on the “reduced” surface than the five-coordinate  $\text{Sn}^{4+}$  cations seen on both the “reduced” and nearly-stoichiometric surfaces.

### ***2.4.3 Acid/Base considerations***

In simple acid/base terms,  $\text{NH}_3$  is considered a hard base [25,26]. The  $\text{Sn}^{4+}$  cations are generally considered hard acids while  $\text{Sn}^{2+}$  cations are thought of as borderline between hard and soft [25,26]. Hard acids and bases tend to be small and slightly polarizable, and soft acids and bases tend to be larger and more polarizable [26]. Density functional calculations show a broad distribution of surface states in the gap for a “reduced” surface occupied by electrons left by removed bridging oxygen anions [27]. Energy of these surface states is strongly influenced by the high polarizability of the  $\text{Sn}^{2+}$  cation [27].

A general rule for acid/base complexes is that hard bases prefer to interact with hard acids due to strong “charge-controlled” or electrostatic interactions, and soft bases prefer soft acids due to “frontier-controlled” or covalent interactions [25,26]. Therefore in simple acid/base terms,  $\text{NH}_3$ , a hard base, should interact more strongly with  $\text{Sn}^{4+}$  cations, which are generally considered harder acids than  $\text{Sn}^{2+}$  cations. The experimental data shows the opposite trend. One obvious difficulty with these comparisons is that the general expectations of acid/base properties based on oxidation states for ions and complexes in solution may not be directly applicable to cations of various coordinations and oxidation states at the surface of an oxide lattice. However, acid/base considerations may not be the best way to think about the  $\text{NH}_3$  interactions with  $\text{SnO}_2$  since they do not

provide a simple explanation as to why  $\text{NH}_3$  interacts more strongly with surface  $\text{Sn}^{2+}$  cations. Since the data indicates a dominant covalent interaction, considerations based on orbital overlap of the  $\text{NH}_3$  lone-pair  $3a_1$  orbital with the cation electronic states may be more fruitful than acid/base descriptions.

Methanol adsorption and dissociation previously reported on  $\text{SnO}_2$  shows a similar trend to the heats of  $\text{NH}_3$  adsorption on the  $\text{SnO}_2$  surfaces. Methanol dissociation to methoxide was found to be dependent on the condition of the Sn cations. Methanol dissociated most readily on the four-coordinate  $\text{Sn}^{2+}$  cations, which are present in the highest abundance on the “reduced” surface than the five-coordinate  $\text{Sn}^{4+}$  cations [15]. The four-coordinate  $\text{Sn}^{2+}$  cations also have a larger heat of  $\text{NH}_3$  adsorption than the five-coordinate  $\text{Sn}^{4+}$  cations. The similar trend suggests that  $\text{NH}_3$  probes some property of the surface cations that may be important for methanol adsorption and dissociation. The correlation between the apparent acidity and methanol dissociation suggests that the dissociation of this weak Brønsted acid occurs at surface sites of highest acidity, but the strength of the  $\text{NH}_3$ –cation interactions is difficult to understand in simple acid/base terms. So, other contributing factors related to covalent bond formation and orbital overlap may be more important than acidity in understanding the similarities on  $\text{SnO}_2$  (110).

One similarity between the electronic properties of methanol and  $\text{NH}_3$  is that both have lone pair of electronic states available to interact with surface Sn cations. For  $\text{NH}_3$ , the  $3a_1$  lone pair interacts with electronic states at the four-coordinate  $\text{Sn}^{2+}$  5s and 5p derived states. To facilitate OH bond cleavage in methanol to form a surface methoxide, methanol is expected to interact through the OH group. The methanol 7A' and 2A'' MOs associated with the two oxygen lone pairs on the OH group may also interact stronger at

the 5s and 5p derived states of the  $\text{Sn}^{2+}$  cations [28]. One possible explanation for the similar behavior between  $\text{NH}_3$  adsorption and methanol dissociation on  $\text{SnO}_2$  is that  $\text{Sn}^{2+}$  cations may form stronger covalent bonds with  $\text{NH}_3$  and methanol due to greater molecular overlap with the lone pairs.

#### ***2.4.4 Differences in desorption temperatures from $\text{Sn}^{4+}$ TDS site***

Differences in desorption temperatures from the  $\text{Sn}^{4+}$  TDS site between the nearly-stoichiometric surface and the “reduced” surface are not well understood.  $\text{Sn}^{4+}$  cations have a higher heat of adsorption on the “reduced” surface compared to the nearly-stoichiometric surface. Density Functional Theory is currently being used to investigate the interaction of  $\text{NH}_3$  at various types of cation sites on  $\text{SnO}_2(110)$  in the hopes of providing insights into the apparent variation in the properties of  $\text{Sn}^{4+}$  sites with variations in surface conditions [29].

#### ***2.4.5 Effects of in-plane oxygen vacancies***

Differences in TDS temperatures were observed between the “highly-defective” surface and the “reduced” surface due to the introduction of in-plane oxygen vacancies on the “highly-defective” surface. The “highly-defective” surface gives two TDS features, but the temperatures of the features are decreased by 70-105 K compared to the “reduced” surface. A model for charge neutrality at oxygen vacancies can be used to help explain the differences in TDS temperatures. If in-plane oxygen vacancies are thought of as color centers, the removal of a neutral oxygen atom from an in-plane position leaves two electrons bound to the vacancy to maintain charge neutrality. Such descriptions of in-

plane oxygen vacancies on SnO<sub>2</sub> (110) have been given elsewhere [12,13,30]. The heat of adsorption of NH<sub>3</sub> might be decreased if the charge in the color center (i.e., in-plane oxygen vacancy) increases the effective electron density of the neighboring cations.

## 2.5 Conclusions

NH<sub>3</sub> appears to be a good probe of Sn cations on SnO<sub>2</sub> (110) surfaces. Based on NH<sub>3</sub> heats of adsorption, four-coordinate Sn<sup>2+</sup> cations at bridging oxygen vacancies on the “reduced” surface appear to be more acidic than five-coordinate Sn<sup>4+</sup> cations. The stronger interactions with Sn<sup>2+</sup> cations are attributed to a predominant covalent contribution to the NH<sub>3</sub>-Sn bond. The Lewis acidity of the Sn cations based on NH<sub>3</sub> heats of adsorption goes through a maximum for the formation of a “reduced” surface as the surface becomes more oxygen deficient, and a similar trend is seen in the extent of dissociation of methanol. Four-coordinate Sn<sup>2+</sup> cations form stronger covalent bonds with NH<sub>3</sub> and methanol due to greater molecular overlap with lone pairs available on both molecules. The introduction of in-plane oxygen vacancies on the “highly-defective” surface reduces the heats of adsorption of the associated cations possibly due to a higher electronic charge density around the cation associated with in-plane oxygen vacancies.

## 2.6 References

---

- [1] K. Tanabe, Solid Acids and Bases (Academic Press, New York, 1970).
- [2] Mamoru Ai, *J. Catal.*, **54** (1978) 426.
- [3] M.A. Barteau, *J. Vac. Sci. Technol. A*, **11** (1993) 2162.
- [4] P.C. Stair, *J. Am. Chem. Soc.*, **104** (1982) 4044.
- [5] J.M. Vohs and M.A. Barteau, *Surf. Sci.*, **176** (1986) 91.
- [6] J.M. Vohs and M.A. Barteau, *J. Phys. Chem.*, **91** (1987) 4766.
- [7] J.M. Vohs and M.A. Barteau, *Surf. Sci.*, **201** (1988) 481.
- [8] M.A. Barteau and J.M. Vohs, in: Successful Design of Catalysts, Ed. T. Inui (Elsevier, Amsterdam, 1988) p.89.
- [9] J.M. Vohs and M.A. Barteau, *Surf. Sci.*, **221** (1989) 590.
- [10] J.M. Vohs and M.A. Barteau, *J. Phys. Chem.*, **95** (1991) 297.
- [11] M.A. Barteau, *J. Vac. Sci. Technol. A*, **11** (1993) 2162.
- [12] D.F. Cox, T.B. Fryberger, and S. Semancik, *Phys. Rev. B*, **38** (1988) 2072.
- [13] D.F. Cox, T.B. Fryberger, and S. Semancik, *Surf. Sci.*, **224** (1989) 121.
- [14] D.F. Cox and T.B. Fryberger, *Surf. Sci.*, **227** (1990) L105.
- [15] V.A. Gercher, D.F. Cox and J.-M. Themlin, *Surf. Sci.*, **306** (1994) 279.
- [16] P.A. Redhead, *Vacuum*, **12** (1962) 203.
- [17] G.A. Somorjai, Introduction to Surface Chemistry and Catalysis (John Wiley & Sons, Inc., New York, 1994).
- [18] A. Many, Y. Goldstein, and N.B. Grover, Semiconductor Surfaces (American Elsevier Publishing, New York, 1971).
- [19] P. Turkes, Ch. Pluntke, and R. Helbig, *J. Phys. C: Solid St. Phys.*, **13** (1980) 4941.
- [20] C.G. Fonstad and R.H. Rediker, *J. Appl. Phys.*, **42** (1971) 2911.
- [21] D.W. Turner, C. Baker, A.D. Baker, and C.R. Brundle, Molecular Photoelectron Spectroscopy (Wiley-Interscience, New York, 1970) 365.
- [22] John C. Kotz and Keith F. Purcell, Chemistry and Chemical Reactivity (Saunders College Publishing, New York, 1987).
- [23] J. Lin, P.M. Jones, M.D. Lowery, R.R. Gay, S.L. Cohen, and E.I. Solomon, *Inorg. Chem.*, **31** (1992) 686.
- [24] J. A. Rodriguez and C.T. Campbell, *Surf. Sci.*, **194** (1988) 475.
- [25] J. Fraissard and L. Petrakis, Acidity and Basicity of Solids (Kluwer Academic Publishers, Boston, 1994).
- [26] J.E. Huheey, E.A. Keiter, and R.L. Keiter, Inorganic Chemistry: Principles of Structure and Reactivity (HarperCollins College Publishers, New York, 1993).
- [27] I. Manassidis, J. Goniakowski, L.N. Kantorovich, and M.J. Gillan, *Surf. Sci.*, **339** (1995) 258.
- [28] W.L. Jorgensen and L. Salem, The Organic Chemist's Book of Orbitals (Academic Press, New York, 1973).
- [29] D.F. Cox and D.M. Teter, unpublished.
- [30] F.H. Jones, R. Dixon, J.S. Foord, R.G. Egdell, and J.B. Pethica, *Surf. Sci.*, **376** (1997) 367.